Inorganic Chemistry

Article

pubs.acs.org/IC

Synthesis, Crystal and Electronic Structure of the Quaternary Magnetic $EuTAl_4Si_2$ (T = Rh and Ir) Compounds

Arvind Maurya,[†] Arumugam Thamizhavel,[†] Alessia Provino,[‡,§] Marcella Pani,[‡,§] Pietro Manfrinetti,[‡,§] Durga Paudyal,[∥] and Sudesh Kumar Dhar*[,†]

[†]Department of Condensed Matter Physics and Materials Science, Tata Institute of Fundamental Research, Colaba, Mumbai 400005, India

[‡]Department of Chemistry, University of Genova, Via Dodecaneso 31, 16146 Genova, Italy

[§]Institute SPIN-CNR, Corso Perrone 24, 16152 Genova, Italy

[∥]The Ames Laboratory, U.S. Department of Energy, Iowa State University, Ames, Iowa 50011-3020, United States

Supporting Information

ABSTRACT: Single crystals of the quaternary europium compounds $EuRhAl_4Si_2$ and $EuIrAl_4Si_2$ were synthesized by using the Al−Si binary eutectic as a flux. The structure of the two quaternary compounds has been refined by single crystal X-ray diffraction. Both compounds are stoichiometric and adopt an ordered derivative of the ternary KCu_4S_3 structure type (tetragonal $tP8$, $P4/mmm$). The two compounds reported here represent the first example of a quaternary and truly stoichiometric 1:1:4:2 phase crystallizing with this structure type. In light of our present results, the structure of the $BaMg_4Si_3$ compound given in literature as representing a new prototype is actually isotypic with the KCu_4S_3 structure. Local spin density approximation including the Hubbard U parameter (LSDA + U) calculations show that Eu ions are in the divalent state, with a significant hybridization between the Eu 5d, Rh (Ir) 4d (5d), Si 3p and Al 3p states. Magnetic susceptibility measured along the [001] direction confirms the divalent nature of the Eu ions in $EuRhAl_4Si_2$ and $EuIrAl_4Si_2$, which order magnetically near ∼11 and ∼15 K, respectively.

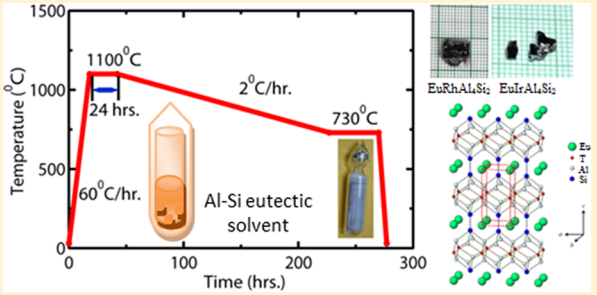

1. INTRODUCTION

The synthesis of new intermetallic phases using metal fluxes is an attractive route when the more common preparation techniques would be difficult to use, or would fail.[1−3] Using this method, it is possible to grow large single crystals of intermetallic compounds having complex structures in some cases, that otherwise would not form due to a variety of reasons such as the high melting point of the starting constituent(s) or the strong volatility of an element due to its high vapor pressure. Despite the fact that Ga, In and Sn are the most commonly utilized metals as fluxes (solvents), the choice of Al flux may become preferable for the synthesis of compounds involving highly oxidizing metals (i.e.: alkaline earths, or the rare earths La, Ce, Eu), thanks to the strong reducing character of liquid Al.

Several quaternary rare earth-based compounds grown from the aluminum flux are known in the literature. For example, $RNiAl_4(Ni_xSi_{2-x})$, $EuNiAl_4Si_2$, $R_2NiAl_4Ge_2$, $RNiAl_4Ge_2$, $RAuAl_4Ge_2$, $RAuAl_4(Au_xGe_{1-x})_2$, $R_8Ru_{12}Al_{49}Si_9(Al_xSi_{12-x})$ and $R_4Fe_{2-x}Al_{7-x}Si_8$, where R is a rare earth metal.[4−6] In some cases, the formation of the compound appears to be dependent on the size of the rare earth element R. While most of the 1:1:4:2 stoichiometric compounds listed above adopt the rhombohedral $YNiAl_4Ge_2$-type structure ($hR24$, space group $R-3m$, No. 166),[7] the phases $RAuAl_4(Au_xGe_{1-x})_2$ and $EuAu_{1.95}Al_4Ge_{1.05}$ crystallize in the tetragonal KCu_4S_3-type structure ($tP8$, space group $P4/mmm$, No. 123),[8,9] or in a supercell derived from this type in the case of the RAu_2Al_4Si compounds ($tP16$, space group $P4/nmm$, No. 129).[6] A common feature of these structures is the presence of slabs "TAl_4X_2" (T = d-transition metal and X = Si or Ge) stacked along the c-axis and alternating with the layer of R atoms.

We have recently focused our attention on the synthesis of Eu-based single crystals and their magnetic properties. In this regard we were able to successfully grow the single crystals of non-centrosymmetric $EuPtSi_3$ and $EuPtGe_3$, using Sn as a solvent.[10,11] By adopting the same experimental protocol, it was not possible to obtain the single crystals of $EuTSi_3$ (T = Rh and Ir). When we used an alternative flux of binary eutectic Al−Si (Al:Si = 87.8:12.2 atomic ratio), which has a relatively low melting point of 577 °C, we obtained the single crystals of $EuTAl_4Si_2$ (T = Rh and Ir). The structural analyses presented in this manuscript show that $EuTAl_4Si_2$ compounds (T = Rh and Ir) crystallize in an ordered derivative of the tetragonal KCu_4S_3-type structure. Electronic structure calculations show

Received: September 18, 2013
Published: January 22, 2014

   dx.doi.org/10.1021/ic402363s | Inorg. Chem. 2014, 53, 1443−1448

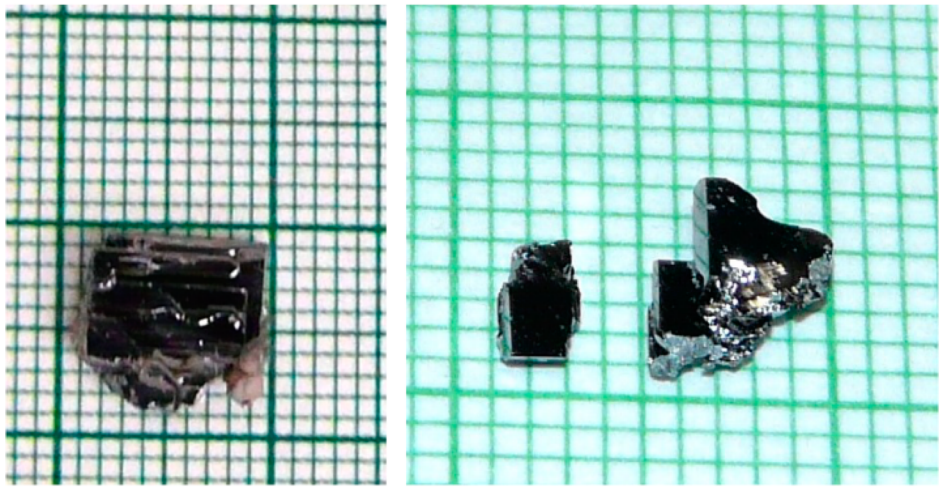

Figure 1. Photographs of single crystals of $EuRhAl_4Si_2$ and $EuIrAl_4Si_2$, grown from eutectic Al−Si flux.

that Eu ions are in the divalent state. Preliminary susceptibility data confirm the theoretical prediction and reveal that $EuRhAl_4Si_2$ and $EuIrAl_4Si_2$ order magnetically at ∼11 and ∼15 K, respectively.

2. EXPERIMENTAL DETAILS

2.1. Reagents and Single-Crystal Growth. Starting metals used in the syntheses were as follows: distilled Eu (99.9 wt % purity), Rh and Ir in powder form (99.9 wt % purity), Al and Si in the form of chunks (99.999 wt % purity). High-temperature solution growth technique was utilized to grow the aforementioned single crystals. These crystals were first formed while attempting to grow 'EuRhSi$_3$" and "EuIrSi$_3$" in Al−Si eutectic composition, though we have verified that they also form starting with the 1:1:4:2 stoichiometry as well. In order to prepare a uniform eutectic mixture of Al−Si, Al and Si were taken in the molar ratio 87.8:12.2 in an alumina crucible (with inner diameter ∼12 mm), sealed in an evacuated quartz ampule and kept at 1100 °C for 48 h. Ingot samples of "EuRhSi$_3$" and "EuIrSi$_3$" were prepared by arc-melting. The combined charge of $EuTSi_3$ (T = Rh and Ir) and the excess of homogenized Al−Si eutectic alloy, taken in 1:8 weight ratio (polycrystal: flux), was placed in a recrystallized alumina crucible, sealed in a quartz ampule at 10^{-6} mbar vacuum and kept inside a PID controlled Carbolite box type furnace. The temperature of the furnace was raised to 1100 °C and maintained for 24 h as soaking period to homogenize the molten mixture inside the alumina crucible; then the temperature was gradually reduced down to 730 °C at the rate of 2 °C/h. Excess Al−Si eutectic flux was centrifuged out at 730 °C before cooling down to room temperature. Some trace amount of the flux, still sticking to the crystal surface, was etched away by dilute hydrochloric acid (HCl). The grown crystals are found to be stable in dilute HCl except for the loss of luster at the mirror-finished surfaces. These compounds also formed when we started with $EuRhAl_4Si_2$ and $EuIrAl_4Si_2$ polycrystalline ingots (though not single phase) as the initial charge instead of $EuTSi_3$ (keeping the remaining conditions identical), thus indicating $EuTAl_4Si_2$ (T = Rh, Ir) as the most stable phase in the present flux. Figure 1 shows the as grown single crystals of $EuTAl_4Si_2$ which have platelet like morphology.

2.2. EDX and X-ray Diffraction. Semiquantitative analysis of several single crystals was performed using a scanning electron microscope (SEM) equipped with an EDX detector (electron dispersive X-ray analysis); a counting time of 50 s was used. The crystals were glued on a SEM-stub by using a carbon tape. X-ray powder patterns were recorded on a PANalytical diffractometer (Ni-filtered Cu Kα radiation). Precise lattice parameters were obtained from Guinier powder patterns (graphite monochromated Cu Kα1 radiation; Si as internal standard, a = 5.4308 Å) by least-squares fits of the pattern readings. Single-crystal intensity data were collected at 293 K for both $EuRhAl_4Si_2$ and $EuIrAl_4Si_2$ compounds on a Bruker-Nonius MACH3 diffractometer, using graphite-monochromated Mo Kα radiation (λ = 0.71073 Å).

2.3. Magnetic Susceptibility. Magnetic susceptibility data were measured between 1.8 and 300 K using a Quantum Design SQUID magnetometer. Oriented samples (typical dimension ∼4 × 2 × 1 mm^3) were fixed on a rectangular thin transparency sheet (∼50 mm × 5 mm) by GE varnish before pushing it inside the standard sample mounting plastic straw commonly used in Quantum Design SQUID magnetometers. The magnetic field is applied along the length of the sample holder.

3. RESULTS AND DISCUSSION

3.1. Crystal Structure. Several crystals were isolated, and their symmetry was checked first by the Laue method. Well-defined Laue diffraction spots, with the 4-fold tetragonal symmetry, clearly indicated a good quality of the grown crystals. The flat plane of the crystal corresponds to the $a-b$ plane. A representative Laue back-reflection diffraction pattern along the c-axis of $EuRhAl_4Si_2$ is shown in Figure S1 (Supporting Information).

In order to find the chemical composition of the crystals, semiquantitative analysis was performed by energy-dispersive X-ray spectroscopy (EDX). In the EDX spectrum, the set of peaks coming from Al and Si (Kα values of 1.486 keV and 1.739 keV, respectively for Al and Si) are well distinguishable, despite the very close atomic number of these two elements. This feature, and then this technique, allowed the elemental composition of the specimen to be measured with good accuracy. The compositions obtained were 12.5:12.5:50:25 atom % for Eu:T:Al:Si (T = Rh and Ir), within 0.6 atom % for each element, and therefore corresponding to an exact stoichiometric ratio of 1:1:4:2. A small portion of a single crystal was ground for X-ray powder diffraction; a representative X-ray diffraction pattern of $EuIrAl_4Si_2$ is shown in Figure 2 along with the Rietveld refinement. The obtained lattice parameters, a and c, are given in Table 1. The formation of the compound leads to a strong volume contraction: ΔV = 14.1 and 13.7% for $EuRhAl_4Si_2$ and $EuIrAl_4Si_2$, respectively (the volume contraction ΔV % is here defined as $\Delta V = [(V_{calc} -$

dx.doi.org/10.1021/ic402363s | Inorg. Chem. 2014, 53, 1443−1448

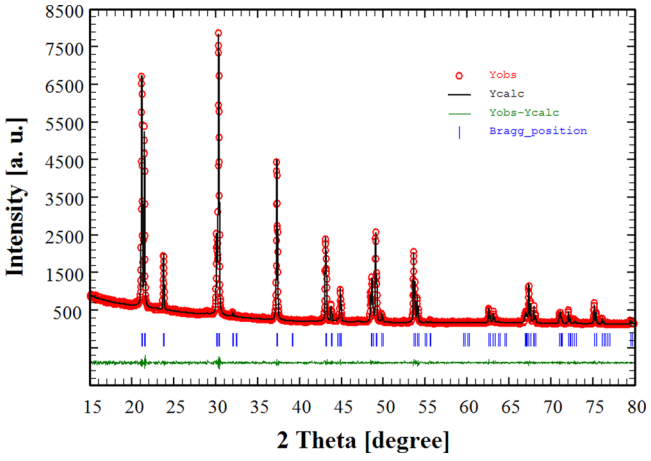

Figure 2. A Rietveld refinement of the X-ray powder pattern of $EuIrAl_4Si_2$ (R_B = 1.17%, R_F = 2.06%, χ^2 = 0.86).

Table 1. Crystal Data and the Details of Data Collection and Structure Refinement for the Examined Single Crystals of $EuRhAl_4Si_2$and $EuIrAl_4Si_2$

Compound	$EuRhAl_4Si_2$	$EuIrAl_4Si_2$
structure prototype	$EuIrAl_4Si_2$	$EuIrAl_4Si_2$
Pearson code	*tP*8	*tP*8
cryst syst	tetragonal	tetragonal
space group, *Z*	*P4/mmm* (No. 123), 1	*P4/mmm* (No. 123), 1
lattice params [Å]	*a* =4.176(1)	*a* = 4.194(1)
	c = 8.289(2)	*c* = 8.269(2)
lattice params[a] [Å]	*a* = 4.1768(2)	*a* = 4.1960(2)
	c = 8.2837(7)	*c* = 8.2711(8)
μ (Mo Kα) [mm^{-1}]	14.5	34.4
calcd density [Mg m^{-3}]	4.81	5.80
cryst size [μm]	25 × 100 × 120	40 × 80 × 140
scan mode	ω–θ	ω–θ
range in *h*, *k*, *l*	±6; ±6; ±12	±6; ±6; ±12
measd reflns	2036	2042
indep reflns	192	193
abs corrn	Gaussian	ψ-scans, 6 reflns
transm ratio (T_{max}/T_{min})	2.73	2.95
refined params	13	13
extinction coeff	0.15(1)	0.088(4)
R1	0.027	0.014
wR2 (F_o^2) all data	0.064	0.039
goodness-of-fit	1.133	1.195
$\Delta\rho_{max}$, $\Delta\rho_{min}$ [e $Å^{-3}$]	+1.75, −4.43	+2.06, −1.43

[a]From Guinier powder pattern.

$V_{obs})/V_{calc}] \times 100$, where V_{calc} is the volume of the compound calculated from the atomic volumes of the individual atoms[12]). In passing from $EuRhAl_4Si_2$ to $EuIrAl_4Si_2$, a slight increase of the lattice parameter *a* and a decrease of the lattice parameter *c* are observed; however, the unit cell volume increases in agreement with the larger atomic dimension of Ir compared with that of Rh. The metallic radii for Ir and Rh are 1.357 Å and 1.345 Å, respectively, for the coordination number CN = 12.[13]

For both $EuRhAl_4Si_2$ and $EuIrAl_4Si_2$ compounds, small fragments from one crushed crystal were checked by Laue patterns, and then the single crystal investigation was performed. The structures of both $EuRhAl_4Si_2$ and $EuIrAl_4Si_2$ were solved with SHELXS-97[14] in the space group *P*/4*mmm* and refined with SHELXL-97.[15] Table 1 shows the crystal data and the details of data collection and structure refinement for the examined single crystals. Table 2 and Table 3 report the

Table 2. Fractional Atomic Coordinates and Equivalent Displacement Parameters for $EuRhAl_4Si_2$, Tetragonal *tP*8, *P4/mmm*, *Z* = 1[a]

atom	Wyckoff site	*x*	*y*	*z*	U_{eq} ($Å^2$)
Atomic Coordinates as in KCu_4S_3 [Eu(K) in Site 1*b*]					
Eu	1*b*	0	0	0.5	0.0088(3)
Rh	1*a*	0	0	0	0.0057(3)
Al	4*i*	0	0.5	0.1680(2)	0.0081(4)
Si	2*h*	0.5	0.5	0.3574(3)	0.0075(5)
Atomic Coordinates as in $BaMg_4Si_3$ [Eu(Ba) in Site 1*a*]					
Eu	1*a*	0	0	0	0.0088(3)
Rh	1*b*	0	0	0.5	0.0057(3)
Al	4*i*	0	0.5	0.3320(2)	0.0081(4)
Si	2*h*	0.5	0.5	0.1426(3)	0.0075(5)

[a]Atomic coordinates are reported placing Rh or Eu, respectively, at the origin of the unit cell (site 1*a*).

Table 3. Fractional Atomic Coordinates and Equivalent Displacement Parameters for $EuIrAl_4Si_2$, Tetragonal *tP*8, *P4/mmm*, *Z* = 1[a]

atom	Wyckoff site	*x*	*y*	*z*	U_{eq} ($Å^2$)
Atomic Coordinates as in KCu_4S_3 [Eu(K) in Site 1*b*]					
Eu	1*b*	0	0	0.5	0.0098(2)
Ir	1*a*	0	0	0	0.0059(2)
Al	4*i*	0	0.5	0.1670(2)	0.0083(4)
Si	2*h*	0.5	0.5	0.3578(3)	0.0082(5)
Atomic Coordinates as in $BaMg_4Si_3$ [Eu(Ba) in Site 1*a*]					
Eu	1*a*	0	0	0	0.0098(2)
Ir	1*b*	0	0	0.5	0.0059(2)
Al	4*i*	0	0.5	0.3330(2)	0.0083(4)
Si	2*h*	0.5	0.5	0.1422(3)	0.0082(5)

[a]Atomic coordinates are reported placing Ir or Eu, respectively, at the origin of the unit cell (site 1*a*).

fractional atomic coordinates and the equivalent displacement parameters for $EuRhAl_4Si_2$ and $EuIrAl_4Si_2$, respectively, while the anisotropic displacement parameters U_{ij} are listed in Table S1 (Supporting Information). Despite the fact that Al and Si differ only by one electron, they could unambiguously be identified during the structure refinements. In both crystals worse or unrealistic displacement parameters were obtained by interchange of Al and Si in the 4*i* and 2*h* positions (wR2 = 0.039 for Al in 4*i* and Si in 2*h* and wR2 = 0.043 for Al in 2*h* and Si in 4*i* for Ir compound; wR2 = 0.064 for Al in 4*i* and Si in 2*h* and 0.077 for Al in 2*h* and Si in 4*i* for Rh compound). Further attempts to refine mixed occupancy gave in general worse thermal parameters, higher esd values or unstable refinements. For each compound the atomic positions for both the KCu_4S_3-type setting [Eu(K) in site 1*b* *(0,0,1/2)*] and for the $BaMg_4Si_3$-type setting [Eu(Ba) in site 1*a* *(0,0,0)*] are respectively given. Table 4 reports the interatomic distances in both the compounds. The structure of the quaternary $EuRhAl_4Si_2$ and $EuIrAl_4Si_2$ is an ordered derivative of the ternary KCu_4S_3-type (tetragonal *tP*8, space group *P4/mmm*, No. 123),[8,9] where Eu, Al and Si occupy the K (1*a*), Cu (4*i*) and S2 (2*h*) Wyckoff sites respectively, while Rh (Ir) sits in the S1 position (1*a*), thus allowing a completely ordered distribution of the four kinds of

dx.doi.org/10.1021/ic402363s | Inorg. Chem. 2014, 53, 1443−1448

Table 4. Interatomic Distances in $EuRhAl_4Si_2$ and $EuIrAl_4Si_2$ [Å]

	$EuRhAl_4Si_2$			$EuIrAl_4Si_2$	
Eu	−8 Si	3.181(1)	Eu	−8 Si	3.190(1)
	−8 Al	3.455(2)		−8 Al	3.461(2)
	−4 Eu	4.176(1)		−4 Eu	4.194(1)
Rh	−8 Al	2.510(1)	Ir	−8 Al	2.511(1)
Al	−2 Rh	2.510(1)	Al	−2 Ir	2.511(1)
	−2 Si	2.613(2)		−2 Si	2.625(2)
	−Al	2.784(4)		−Al	2.761(4)
	−4 Al	2.953(1)		−4 Al	2.966(1)
	−2 Eu	3.455(2)		−2 Eu	3.461(2)
Si	−Si	2.364(5)	Si	−Si	2.351(6)
	−4 Al	2.613(2)		−4 Al	2.625(2)
	−4 Eu	3.181(1)		−4 Eu	3.190(1)

atoms and the fixed 1:1:4:2 stoichiometry. All the crystallographic sites are fully occupied, with no mixed occupations.

Even though several compounds having a structure derived from the KCu_4S_3-type are known, to our knowledge this appears to be the first case of a completely ordered quaternary derivative of this structure type and therefore represents a new quaternary structural prototype. Moreover, a survey of the existence of ternary structural prototypes does not highlight the formation of any other prototype on the 1:4:3 stoichiometry.

A sketch of the crystal structure for the $EuIrAl_4Si_2$ compound, along the [*010*] direction, is shown in Figure 3.

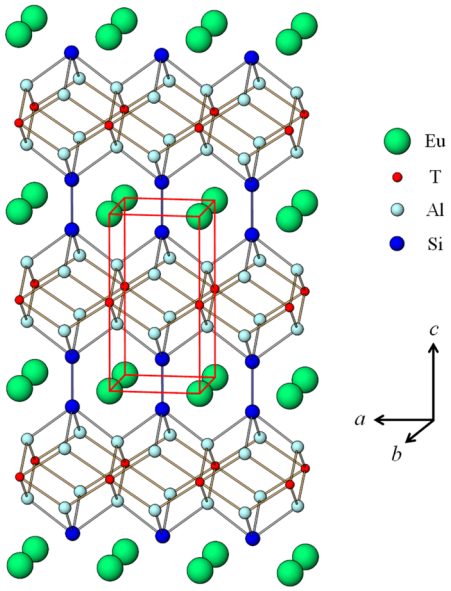

Figure 3. A sketch of the crystal structure of $EuTAl_4Si_2$, T = Rh, Ir: view of the structure along the [*010*] direction; Eu−Eu, Eu−Si and Eu−Al bonds are not shown for simplicity.

The crystal structure of the two compounds is built up by two-dimensional frameworks of $[TAl_4Si_2]$ linked to each other by Si−Si bonds along the *c* direction, giving rise to a tridimensional arrangement in which Eu atoms fill the empty spaces. Eu is an electropositive lanthanide element; on the other hand, it must be recalled here that the T atoms, Rh and Ir, with their electronegativity values of 2.28 and 2.20 (Pauling scale), respectively, are the most electronegative elements in the structure (even more electronegative than Si, with a value of 1.90). This may likely bring a higher electron density onto the T atoms at the center of the $[TAl_4Si_2]$ slabs. The higher electronegativity of the T metals might be one, but not the only, factor determining the formation of a truly ordered structure. It may be noted that for T = Au (2.54), which is even more electronegative than Rh and Ir, the $EuAu_{1.95}Al_4Si_{1.05}$[6] and $EuAuAl_4(Au_{0.4}Ge_{0.6})_2$[5] phases, and not the ordered "$EuAuAl_4Si_2$" and "$EuAuAl_4Ge_2$", are formed. The dimensional factor could also play a strong role. In this regard, the atomic volume of Au (16.97 $Å^3$) is larger than the atomic volume of either Rh or Ir (13.67 $Å^3$ and 14.14 $Å^3$, respectively); it is comparable to that of Al (16.60 $Å^3$), and closer to that of Si (20.02 $Å^3$). However, the dimensional factor still may not play the most important role because, instead of the above $EuAuAl_4(Au_xSi_{1-x})_2$ and/or $EuAuAl_4(Au_xGe_{1-x})_2$ compounds, phases like $EuAu(Au_xAl_{1-x})_4Si_2$ (with mixed Au/Al occupancy) would have formed. Therefore, besides the number of valence electrons, the concurrent effect of both electronegativity and atomic size brings about the formation of these stoichiometric $EuTAl_4Si_2$ phases.

The Eu atoms are arranged in a flat "square-net", with Eu−Eu distances equal to the *a* cell parameter (4.194 Å). All of the Eu atoms are inside a cage formed by 8 Si atoms at a bond distance of 3.190 Å; however, 8 more Al atoms at a distance of 3.461 Å can still be considered to give a global coordination number CN = 16 for each Eu atom (Figure 4a). The Ir atoms

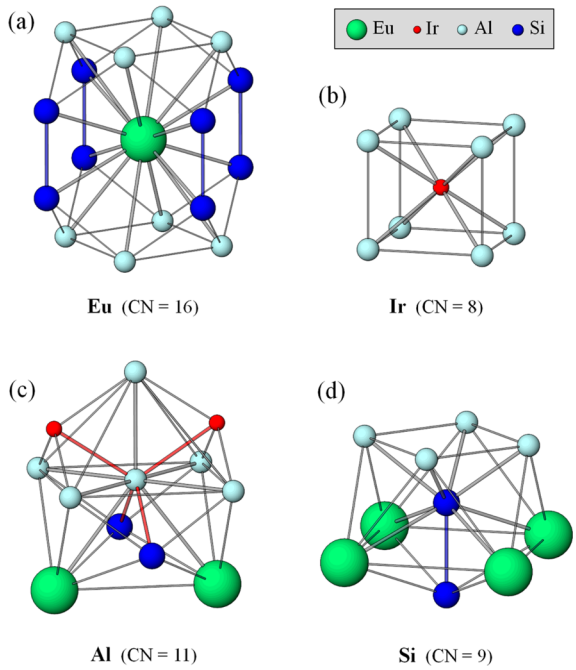

Figure 4. Coordination polyhedra of Eu (a), Ir (b), Al (c) and Si (d) atoms.

are arranged in a square network (whose edge is 2.996 Å), where each one is sitting inside a slightly distorted cube (2.966 × 2.966 × 2.761 $Å^3$) formed by 8 Al atoms (CN = 8) (Figure 4b); these cubes share with each other their edges with Al−Al bond distances of 2.761 Å, to form infinite slabs. The first coordination shell of Al atoms has tetrahedral geometry, with 2 Si and 2 Ir atoms at the tetrahedron vertices (d_{Al-Si} = 2.625 Å, d_{Al-Ir} = 2.511 Å); however, other 5 Al and 2 Eu atoms pertain to the coordination polyhedron around the Al (CN = 11, Figure 4c). The Si atoms form Si−Si pairs with very short Si−Si bond distance of 2.351 Å. This distance, being identical to that

dx.doi.org/10.1021/ic402363s | *Inorg. Chem.* 2014, 53, 1443−1448

in elemental Si ($cF8$, $Fd\bar{3}m$)], leads to a strong chemical bond with covalent character, which contributes to a tight bonding of the [TAl_4Si_2] slabs to each other (Figure 3). Each Si−Si pair is placed inside a square of 4 Eu atoms. Each of the two Si atoms is linked also to 4 Al atoms (2.625 Å) to form a square antiprism monocapped by the second Si atom of the pair; the coordination polyhedron of each Si atoms is shown in Figure 4d. The coordination polyhedra around the Eu, Ir and Si atoms are also shown in Figure 5, where their tridimensional stacking

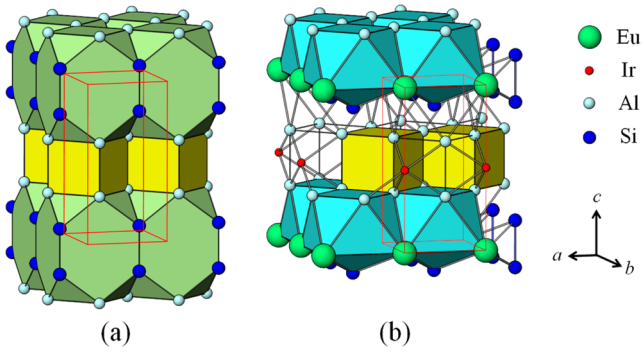

Figure 5. Projection of the structure where the polyhedra around Eu (green) and Ir (yellow) atoms (a) and around Ir (yellow) and Si (blue) atoms (b) are highlighted.

is highlighted. All the shortest interatomic distances mentioned above are well comparable to those found in the binary and ternary compounds such as $EuSi_2$ ($ThSi_2$-type, $tI12$), $EuAl_2Si_2$ ($CaAl_2Si_2$-type, $hP5$) and $EuIr_2Si_2$ ($ThCr_2Si_2$-type, $tI10$).[16]

A survey of the literature data on the existing 1:4:3 and 1:1:4:2 phases, with a similar primitive tetragonal unit cell ($tP8$, $P4/mmm$, $Z = 1$) suggests the reported $BaMg_4Si_3$-type[17] as a further possible prototype for the present $EuTAl_4Si_2$ compounds. The $BaMg_4Si_3$ structure type has been reported as a prototype for the $BaMg_4Ge_3$[17] and, more recently, for $EuCu_4P_3$[18] compounds. However, from a comparison between the two structures KCu_4S_3 and $BaMg_4Si_3$, it is well evident that the $BaMg_4Si_3$-type, reported as a new structure type, is actually corresponding to the KCu_4S_3-type: by shifting the origin of the unit cell by [*0 0 1/2*] the two structures are in fact the same. For this reason in Tables 2 and 3 two different and equivalent settings of the atomic positions are given. More detailed discussions about the structure of the ternary parent KCu_4S_3-type, the $BaMg_4Si_3$ structure type and of quaternary phases having similar structures, can be found in refs 5, 6, 9 and 17.

3.2. Magnetic Susceptibility. Figure 6 shows the magnetic susceptibility data between 300 and 1.8 K in an applied field of 1 kOe for the two compounds, with the magnetic field applied along the [*001*] direction. The inverse susceptibility follows the Curie−Weiss law, and a least-squares fitting algorithm furnishes a paramagnetic effective moment, μ_{eff} of (7.834 ± 0.005) and (7.904 ± 0.001) μ_B for $EuRhAl_4Si_2$ and $EuIrAl_4Si_2$, respectively; these values are comparable to the Hund's rule derived value of 7.94 μ_B for the free-ion Eu^{2+}. The divalent Eu ions in the two compounds should order magnetically at temperatures determined by the strength of the oscillatory RKKY (Ruderman−Kittel−Kasuya−Yosida) exchange interaction.[20−22] The inset of Figure 6 shows the field cooled magnetization in 50 Oe and below 20 K. A magnetic transition near 11 and 15 K is observed in $EuRhAl_4Si_2$ and $EuIrAl_4Si_2$, respectively. Detailed investigation of the magnetic properties of these two crystals,

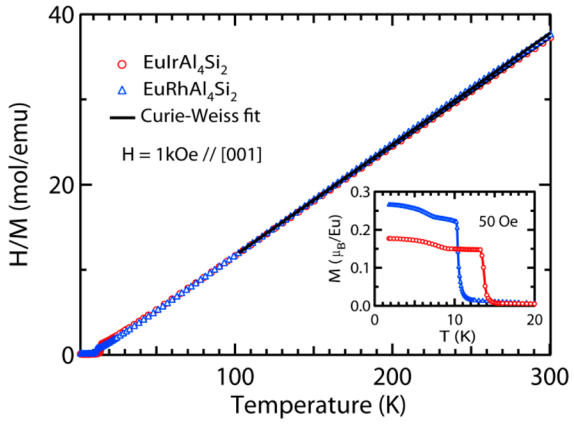

Figure 6. The inverse magnetic susceptibility, H/M, of $EuTAl_4Si_2$ (T = Rh, Ir) between 1.8 and 300 K in H = 1 kOe field. The inset shows the magnetic transition recorded in the field cooled magnetization M below 20 K and in H = 50 Oe.

probed by the magnetization, heat capacity, electrical resistivity and ^{151}Eu Mössbauer spectroscopy, is currently under study and will be reported elsewhere.

4. THEORETICAL CALCULATIONS

Local spin density approximation including the Hubbard, U parameter (LSDA + U) calculations have been performed using the tight-binding linear muffin tin orbital band structure method.[19] The conventional von Barth and Hedin exchange correlation potentials have been used. A total of 2601 irreducible k-points from 32 × 32 × 32 Brillouin zone mesh have been used for k-space integration. We have used intra-atomic Coulomb correlation U = 6.7 eV and exchange interaction J = 0.7 eV in these calculations.

Figure 7 shows atom projected density of states (DOS) of $EuRhAl_4Si_2$ and $EuIrAl_4Si_2$ compounds. The 4f states of Eu in

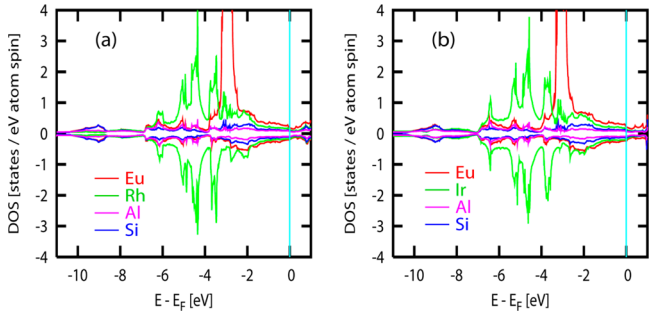

Figure 7. The atom projected density of states (DOS) of $EuRhAl_4Si_2$ and $EuIrAl_4Si_2$ compounds. The density of states above and that below the zero level represent spin up and spin down density of states. The negative numbering in the spin down direction is just the representation of spin down density of states.

both compounds are localized around −3 eV. The total density of states at the Fermi level of $EuIrAl_4Si_2$ is higher by 4.1% compared to that of $EuRhAl_4Si_2$, which may be the reason why the magnetic transition temperature in the former is higher compared to the latter. The 4f magnetic moment of Eu in both compounds is 7 μ_B/Eu, which confirms that the Eu has $4f^7$ (divalent) state. Moreover, in both $EuRhAl_4Si_2$ and $EuIrAl_4Si_2$, we find small but non-negligible spin polarized Eu 5d moment (~0.1 μ_B). This is because of the indirect 4f−4f exchange

dx.doi.org/10.1021/ic402363s | Inorg. Chem. 2014, 53, 1443−1448

interaction. Although the 5d states are not generally considered in the atomic picture of divalent compounds, the calculated 5d density of states of Eu atoms in $EuIrAl_4Si_2$ and $EuRhAl_4Si_2$ indeed shows the role of 5d bands. Because of the Eu 5d and Rh 4d (Ir 5d) hybridization, the non-negligible density of states of Eu 5d originates. Further, a strong hybridization has been observed between Eu 5d, Rh (Ir) 4d (5d), Si 3p, and Al 3p. This hybridization indicates stable band formation and phase stability of these two compounds. Importantly, the Eu 4f and Rh 4d (Ir 5d) are also hybridized at around −3 eV, which may indicate the involvement of small but non-negligible direct 4f and d interactions. Therefore, the contribution of the Eu 5d appears significant in these compounds. Figure 8 shows the 5d density of states (DOS) of Eu in $EuRhAl_4Si_2$ and $EuIrAl_4Si_2$. The 5d densities of states in both compounds are almost identical, indicating a similar electronic structure in these compounds which may arise due to the localized nature of Rh 4d and Ir 5d electrons.

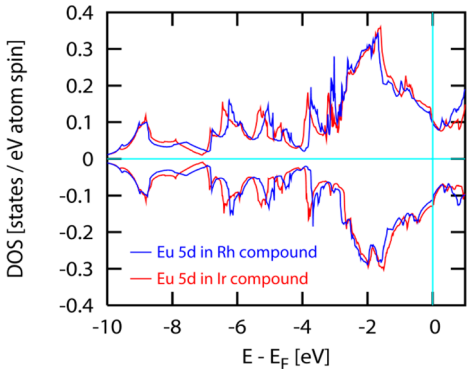

Figure 8. The 5d density of states (DOS) of Eu in $EuRhAl_4Si_2$ and $EuIrAl_4Si_2$ compounds. The density of states above and that below the zero level represent spin up and spin down density of states.

5. CONCLUSION

In conclusion, we report here two new compounds with stoichiometry $EuTAl_4Si_2$ (T = Rh and Ir). There is only one Eu site in the unit cell, and the symmetry-equivalent Eu ions are divalent in both compounds and order magnetically at low temperatures. Efforts are also ongoing to explore the possibility of growing single crystals with other rare earth metals, in particular Ce and Yb.

■ ASSOCIATED CONTENT

Supporting Information

Back-reflection Laue diffraction pattern of a single crystal of $EuRhAl_4Si_2$ (Figure S1), Rietveld refinement data for the $EuIrAl_4Si_2$ compound (Table S1), anisotropic and equivalent displacement parameters for $EuRhAl_4Si_2$ and $EuIrAl_4Si_2$ (Table S2) and crystallographic information file. This material is available free of charge via the Internet at http://pubs.acs.org.

■ AUTHOR INFORMATION

Corresponding Author

*E-mail: sudesh@tifr.res.in.

Notes

The authors declare no competing financial interest.

■ ACKNOWLEDGMENTS

The theory part of the work was supported by the U.S. Department of Energy, Office of Basic Energy Science, Division of Materials Sciences and Engineering. The Ames Laboratory is operated for the U.S. Department of Energy by Iowa State University under Contract No. DE-AC02-07CH11358.

■ REFERENCES

(1) Kanatzidis, M. G.; Pöttgen, R.; Jeitschko, W. *Angew. Chem.* **2005**, *44*, 6996−7023.
(2) Canfield, P. C.; Fisk, Z. *Philos. Mag. B* **1992**, *65*, 1117−1123.
(3) Phelan, W. A.; Menard, M. C.; Kangas, M. J.; McCandless, G. T.; Drake, B. L.; Chan, J. Y. *Chem. Mater.* **2012**, *24*, 409−420.
(4) Sieve, B. Ph.D. Dissertation, Michigan State University, 2002.
(5) Wu, X.; Kanatzidis, M. G. *J. Solid State Chem.* **2005**, *178*, 3233.
(6) Latturner, S. E.; Kanatzidis, M. G. *Inorg. Chem.* **2008**, *47*, 2089.
(7) Sieve, B.; Chen, X.; Cowen, J.; Larson, P.; Mahanti, S. D.; Kanatzidis, M. G. *Chem. Mater.* **1999**, *11*, 2451−2455.
(8) Rudorff, W.; Schwarz, H. G.; Walter, M. *Z. Anorg. Allg. Chem.* **1952**, *269*, 141.
(9) Brown, D. B.; Zubieta, J. A.; Vella, P. A.; Wrobleski, J. T.; Watt, T.; Hatfield, W. E.; Day, P. *Inorg. Chem.* **1980**, *19*, 1945−1950.
(10) Kumar, N.; Dhar, S. K.; Thamizhavel, A.; Bonville, P.; Manfrinetti, P. *Phys. Rev. B* **2010**, *81*, 144414.
(11) Kumar, N.; Das, P. K.; Kulkarni, R.; Thamizhavel, A.; Dhar, S. K.; Bonville, P. *J. Phys.: Condens. Matter* **2012**, *24*, 036005.
(12) Villars, P.; Daams, J. L. C. *J. Alloys Compd.* **1993**, *197*, 177−196.
(13) Teatum, E.; Gschneidner, K. A. Jr.; Waber, J. *Rep. LA-4003*; National Technical Information Service: Springfield, VA, USA, 1968.
(14) Sheldrick, G. M. *SHELXS-97, Program for Crystal Structure Solution*; University of Göttingen: Germany, 1997.
(15) Sheldrick, G. M. *SHELXL-97, Program for Refinement of Crystal Structures*; University of Göttingen: Göttingen, Germany, 1997.
(16) Villars, P.; Cenzual, K. *Pearson's Crystal Data: Crystal Structure Database for Inorganic Compounds (DVD)*; ASM International: Materials Park, OH, USA, release 2012/13.
(17) Zürcher, F.; Wengert, S.; Nesper, R. *Inorg. Chem.* **1999**, *38*, 4567−4569.
(18) Charkin, D. O.; Urmanov, A. V.; Kazakov, S. M.; Batuk, D.; Abakumov, A. M.; Knöner, S.; Gati, E.; Wolf, B.; Lang, M.; Shevelkov, A. V.; Van Tendeloo, G.; Antipov, E. V. *Inorg. Chem.* **2012**, *51*, 8948−8955.
(19) Andersen, O. K.; Jepsen, O. *Phys. Rev. Lett.* **1984**, *53*, 2571.
(20) Ruderman, M. A.; Kittel, C. *Phys. Rev.* **1954**, *96*, 99.
(21) Kasuya, T. *Prog. Theor. Phys.* **1956**, *16*, 45.
(22) Yosida, K. *Phys. Rev.* **1957**, *106*, 893.